Acta Biomaterialia 10 (2014) 709–721

Contents lists available at ScienceDirect

Acta Biomaterialia

journal homepage: www.elsevier.com/locate/actabiomat

Artificial neural network for modeling the elastic modulus of electrospun polycaprolactone/gelatin scaffolds

Elham Vatankhah [a,b], Dariush Semnani [a], Molamma P. Prabhakaran [b,*], Mahdi Tadayon [c], Shahnaz Razavi [d], Seeram Ramakrishna [b,e]

[a] Department of Textile Engineering, Isfahan University of Technology, Isfahan 84156-83111, Iran
[b] Center for Nanofibers and Nanotechnology, E3-05-14, Nanoscience and Nanotechnology Initiative, Faculty of Engineering, National University of Singapore, 2 Engineering Drive 3, Singapore 117576, Singapore
[c] Behrad Consulting Engineers, Isfahan 81367-13833, Iran
[d] Department of Anatomical Sciences and Molecular Biology, School of Medicine, Isfahan University of Medical Sciences, Isfahan 81744-176, Iran
[e] Department of Mechanical Engineering, Faculty of Engineering, National University of Singapore, 2 Engineering Drive 3, Singapore 117576, Singapore

ARTICLE INFO

Article history:
Received 1 March 2013
Received in revised form 29 August 2013
Accepted 8 September 2013
Available online 25 September 2013

Keywords:
Electrospun scaffold
Elastic modulus
Artificial neural network model
Fiber diameter
Orientation

ABSTRACT

Scaffolds for tissue engineering (TE) require the consideration of multiple aspects, including polymeric composition and the structure and mechanical properties of the scaffolds, in order to mimic the native extracellular matrix of the tissue. Electrospun fibers are frequently utilized in TE due to their tunable physical, chemical, and mechanical properties and porosity. The mechanical properties of electrospun scaffolds made from specific polymers are highly dependent on the processing parameters, which can therefore be tuned for particular applications. Fiber diameter and orientation along with polymeric composition are the major factors that determine the elastic modulus of electrospun nano- and microfibers. Here we have developed a neural network model to investigate the simultaneous effects of composition, fiber diameter and fiber orientation of electrospun polycaprolactone/gelatin mats on the elastic modulus of the scaffolds under ambient and simulated physiological conditions. The model generated might assist bioengineers to fabricate electrospun scaffolds with defined fiber diameters, orientations and constituents, thereby replicating the mechanical properties of the native target tissue.

1. Introduction

Providing an alternative to conventional transplants through the development of biomimetic scaffolds is one of the primary objective of tissue engineering (TE) [1]. An ideal TE scaffold, as a simulator of the native extracellular matrix (ECM), should have the physical, biological and mechanical requisites of the target cells. The native ECM is a molecular complex made up of proteins, especially collagen, and polysaccharides, comprising a three-dimensional hierarchical fibrous structure with nanoscale dimensions [2]. Recently nanofibrous scaffolds have received much attention in TE due to their similarity to the fibrillar structure of native ECM, both morphologically and dimensionally [3]. The porous nature of the nanofibers allows cells to migrate into and proliferate in the scaffold, and the transport of nutrients and metabolic waste through the porous nanofibers [4]. Among the various available methods used to fabricate nanofibrous scaffolds, electrospinning remains the most popular technique owing to its simplicity and inexpensive nature, as well as its ability to form nano- and microfibers from a wide range of synthetic and natural polymers. For the fabrication of a bio-scaffold the critical issue for bioengineers is the careful selection of biocompatible polymers with proportional degradability to remodel the tissue concerned.

Polycaprolactone (PCL), a semicrystalline linear hydrophobic polymer, is one of the most commonly used FDA approved polymers that has been electrospun either alone or in combination with other synthetic or natural polymers to fabricate nanofibrous scaffolds for bone, cartilage, nerve, blood vessel, skin, corneal, cardiac, tendon and ligament tissue regeneration. The lack of surface cell recognition sites and poor hydrophilicity of pure PCL scaffolds make them unsuitable for cell adhesion, proliferation, and differentiation and, hence, the blending of PCL with natural polymers such as gelatin and collagen has been used to combine both the mechanical durability of the synthetic component (PCL) and the cell affinity of the natural protein [5].

Although collagen is an adhesion protein present in the native ECM which enables cell attachment and proliferation through

* Corresponding author.
E-mail address: nnimpp@nus.edu.sg (M.P. Prabhakaran).

1742-7061/$ - see front matter
http://dx.doi.org/10.1016/j.actbio.2013.09.015

specific interactions between its RGD domains and integrin receptors in the cell membrane, electrospinning of collagen is an expensive way of making gelatin fibers [6]. Gelatin is a natural biopolymer derived from collagen by controlled hydrolysis and is biocompatible, biodegradable and commercially available at relatively low cost [7].

Electrospun PCL/gelatin scaffolds have been used as substrates for skin, bone, nerve, cardiac, and blood vessel TE by many researchers [5,7–12]. However, the mechanical properties of PCL/gelatin nanofibers require modification so as to mimic the target tissue of regeneration. The mechanical properties of electrospun PCL/gelatin scaffolds is mainly influenced by the ratio of PCL to gelatin [5], but like other electrospun scaffolds it also depends on the orientation [13–15] and diameter of the fibers [14]. A proper understanding of the relationship between these parameters and the macro-mechanical properties of electrospun scaffolds will help bioengineers fabricate optimized scaffolds for any desired purposes primarily by controlling the scaffold composition and architecture.

Artificial neural network (ANN) is a modeling tool to solve linear and nonlinear multivariate regression problems [16]. The massive interconnected structure make ANN an exceptional tool which learns through input data, while it has the ability to model incomplete data without being affected by data noise. Such techniques have proved more efficient than standard modeling techniques such as the response surface methodology (RSM). Various parameters affect the electrospinning process, such as the solution properties and processing conditions, along with other ambient parameters with known or unknown effects on each other, thus making the electrospinning process a complex procedure, which also highlight the need to employ an ANN model instead of classical statistical tools [17]. RSM is a statistical technique commonly utilized to estimate a quadratic model and cannot be applied to complicated cases such as electrospinning. Collinearity of the parameters influencing the electrospinning procedure is another limitation of using RSM modeling for this application [18].

In recent years ANN have been applied to model the electrospinning process, mostly aimed at predicting the diameter of electrospun polyacrylonitrile [19–21], polyethylene oxide [22], polyurethane [23] and nylon-6,6 [17] nanofibers. At the same time an ANN-based model was demonstrated to predict the water retention capacity of electrospun polyacrylonitrile fibers [24]. Although the capability of neural network to model the mechanical properties of materials is well known, particularly those of textile structures [25–27], no attempt has been made until now to apply an ANN-based model to predict the mechanical properties of electrospun fibers. Therefore the main objective of the present study was to develop an ANN-based model to analyze the nonlinear effect of the above mentioned parameters on the elastic modulus of electrospun PCL/gelatin fibers, which is one of the most widely used scaffolds in TE. During this study fibers of different compositions, fiber diameters and orientations were fabricated by combining different weight ratios of PCL and gelatin, with varying total solution concentrations and mandrel rotation speeds, and their relation to the elastic modulus was interpreted using an ANN-based model.

2. Experimental and modeling

2.1. Materials

Polycaprolactone (M_w = 70,000–90,000), gelatin type A (300 Bloom) from porcine skin, 1,1,1,3,3,3-hexafluoro-2-propanol (HFP) and phosphate-buffered saline (PBS) were all purchased from Sigma–Aldrich (Singapore).

2.2. Scaffold fabrication

Polymer solutions with concentrations of 8%, 11%, 14%, and 17% w/v were prepared by dissolving PCL and gelatin at weight ratios of 30:70, 50:50, 70:30, and 90:10 at room temperature with stirring for a period of 22 h. The rotation speed of the collector (rotating mandrel) was set to 50, 200, 700, or 1200 r.p.m. A set of experiments based on a Taguchi L'16 orthogonal array [28,29] was conducted to study the influence of composition, fiber diameter, and fiber orientation on the elastic modulus of electrospun PCL/gelatin scaffolds by changing variable parameters such as the individual polymer weight ratio of PCL to gelatin, total solution concentration, and mandrel rotation speed.

Other electrospinning parameters were kept approximately constant for all the experiments. The polymer solution was electrospun from a 3 ml syringe attached to a 27 G blunted stainless steel needle at a flow rate of 3–5 ml h^{-1}. A positive voltage (10–12 kV) was applied to the polymer solution and the distance between the syringe tip and the mandrel collector was maintained at a distance of 13 cm, while the mandrel length and diameter were 10 and 14 cm, respectively. For a better comparison of the mechanical properties of the nanofibrous mat membrane with a thickness of 60–80 μm was collected for all scaffolds. The collector was regularly moved to ensure a uniform thickness of the scaffold along the length of the mandrel. The electrospinning parameters to prepare different samples according to the Taguchi method are summarized in Table 1.

2.3. Morphological characterization

Structural characterization of the scaffolds was performed using scanning electron microscopy (FEI-Quanta 200F, The Netherlands) at an accelerating voltage of 10 keV, after sputter coating with gold (JEOL JFC-1600 Auto fine coater, Japan). Imaging was carried out in such a manner that the circumferential direction (the direction of mandrel rotation) of the samples was vertical in the images. Fiber diameter and orientation were determined from scanning electron microscopy (SEM) images using image analysis software (ImageJ, National Institutes of Health, Bethesda, MD), with the fiber diameter being the average value of 100 random points in the respective SEM images.

The fiber orientations were evaluated with a novel ImageJ plug-in, OrientationJ [30,31]. Three images per sample were used to quantify the alignment of the nanofibers. The coherency coefficients ranged from 0 to 1, where values close to 0 and 1 refer to random and aligned fibers, respectively [31]. Therefore, two parameters for orientation evaluation were considered, the dominant fiber direction and the coherency coefficient in the dominant direction to demonstrate the direction and intensity of fiber orientation, respectively. The average coherency coefficient is an index of the alignment intensity (alignment index (AI)). To minimize the dominant alignment direction errors arising during placement of the samples on the SEM plate the alignment directions were categorized in 10° increments and the angles were defined relative to the horizontal axis.

2.4. Uniaxial tensile testing

The electrospun scaffolds were dried in a vacuum oven and used for further experiments. The thickness of the specimens was measured using a Mitutoyo digital micrometer. The elastic modulus of the electrospun scaffolds was determined by uniaxial tensile testing of rectangular specimens (30 mm length × 10 mm width) using an Instron 5943 table top tester, with a 50 N load cell and at an extension rate of 10 mm min^{-1}. An algorithm for Young's modulus determination provided by the Bluehill3 software over a

Table 1
Experimental data based on Taguchi's experimental design and the respective fiber diameters, alignment indices and dominant alignments of PCL/gelatin nanofibers.

Sample	Weight ratio PCL:gelatin	Polymer concentration (% w/v)	Rotation speed (r.p.m.)	Fiber diameter (nm)	Alignment index	Dominant alignment direction (°)
1	30:70	8	50	415 ± 33	0.10	80
2	30:70	11	200	580 ± 87	0.26	80
3	30:70	14	700	865 ± 242	0.35	70
4	30:70	17	1200	1195 ± 382	0.30	70
5	50:50	8	200	472 ± 56	0.36	50
6	50:50	11	50	595 ± 107	0.35	10
7	50:50	14	1200	781 ± 234	0.64	80
8	50:50	17	700	1070 ± 374	0.30	80
9	70:30	8	700	270 ± 43	0.51	80
10	70:30	11	1200	400 ± 108	0.60	90
11	70:30	14	50	889 ± 285	0.26	20
12	70:30	17	200	1289 ± 374	0.15	20
13	90:10	8	1200	279 ± 25	0.65	70
14	90:10	11	700	328 ± 66	0.63	70
15	90:10	14	200	620 ± 230	0.22	40
16	90:10	17	50	688 ± 227	0.17	20

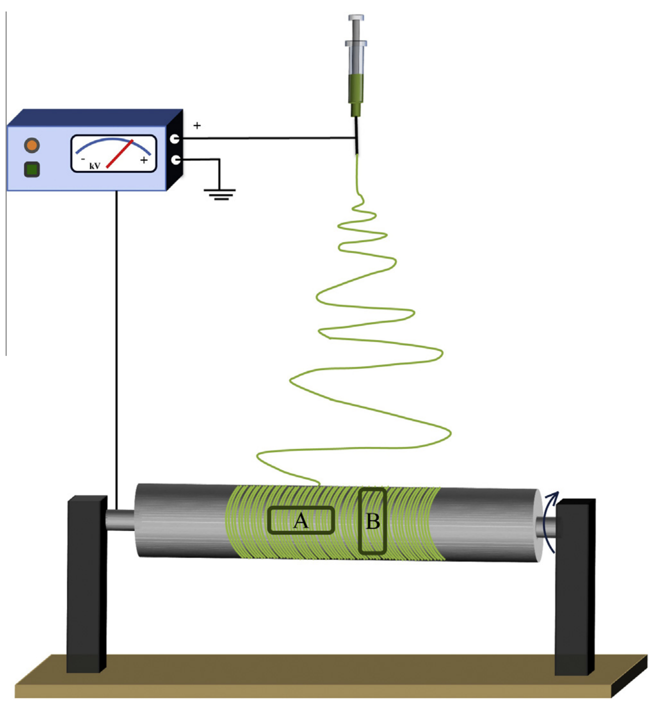

Fig. 1. Schematic diagram of electrospinning in (A) the longitudinal direction (B) the circumferential direction.

strain from 0.1% to 5.0% was used during this test. Mechanical tests were performed on at least five samples in both the circumferential (the direction of mandrel rotation) and longitudinal (perpendicular to the direction of mandrel rotation) directions, as shown in Fig. 1. Mechanical tests were carried out under two different conditions: (1) ambient conditions; (2) simulated physiological conditions (after 24 h incubation in PBS at 37 °C).

To perform the mechanical tests for samples treated under simulated physiological conditions the samples were directly taken out of the PBS and measured immediately under ambient conditions. However, using 5.0% strain for elastic modulus evaluation and an extension rate of 10 mm min^{-1} means the elastic modulus can be estimated in a few seconds time, which means measurement of the elastic modulus was carried out on completely wet samples.

Although dog bone-shaped samples are more appropriate than rectangular samples to mitigate tensile stress at the edges of the samples, we used rectangular samples because the handling of dog bone-shaped samples after hydration, especially samples with a higher gelatin content, was very difficult. In addition, we rarely observed any breakage at the edges of the scaffolds, and if it had happened the results would have been ignored.

2.5. Topology of the neural network model

One critical parameter influencing the predictive power of a neural network model is its topology. However, there is no straightforward method to estimate the optimal number of hidden layers and neurons in each layer [32]. Thus trial and error methods have been used by many researchers to determine such case-dependent parameters for studies involving ANN-based models.

In this research a single hidden layer perceptron feed forward ANN based on a back propagation (BP) algorithm was applied. According to Kolmogorov's theorem, ANN with a single hidden layer should be capable of approximating any function to any degree of accuracy [21,23]. Furthermore, using a trial and error method we observed that "one hidden layer consisting of only one neuron" might present the most accurate predictions with the lowest "mean absolute percentage error" (MAPE) values. The log-sigmoid (Eq. (1)) and hyperbolic tangent sigmoid transfer (Eq. (2)) functions were employed for the hidden and output layers, respectively.

$$f(x) = \frac{1}{1+e^{-x}}, \quad 0 \leqslant f(x) \leqslant 1 \tag{1}$$

$$f(x) = \frac{2}{1+e^{-2x}} - 1, \quad -1 \leqslant f(x) \leqslant 1 \tag{2}$$

2.6. Training and validating the neural network model

Another important point when applying a neural network is avoiding overfitting by proper selection of the training and test data sets.

To obtain more accurate predictions an individual model was designed for each of the following four cases: longitudinal direction under ambient conditions; circumferential direction under ambient conditions; longitudinal direction under simulated physiological conditions; circumferential direction under simulated physiological conditions. The input data for all models were the polymer weight ratio, fiber diameter, and fiber orientation of 16 prepared samples, while the output data was the elastic modulus.

Here a genetic algorithm (GA) was used as a heuristic method to determine the number of samples (between 3 and 5) to serve as the test data set, selecting them from among the 16 samples to prevent overfitting. 50 random groups of training and test data sets (according to the employed samples) were inserted into the GA and 10 ANN models were developed for each group. Prior to starting the network training both the input and output values were normalized.

To improve the model efficiency different learning algorithms, including the Levenberg–Marquardt (LM), Scaled Conjugate Gradient (SCG) and Resilient Back-propagation (RP) methods, were implemented, among which the Levenberg–Marquardt training method was selected because of a better convergence rate and performance of the ANN model.

The MAPE (Eq. (3)) was calculated for each respective group in the training step. Further, using the designed genetic operators the best 20 groups with the minimum MAPE values were obtained to validate the quality of the ANN models over the data from 16 experimental samples through computing the MAPE and linear correlation coefficient (R^2) (Eq. (4)). The best model with the lowest MAPE and highest linear correlation coefficient (R^2) was selected as the final model.

$$\mathrm{MAPE} = \frac{1}{n}\sum_{i=1}^{n} \frac{|y_i - \hat{y}_i|}{y_i} \times 100 \tag{3}$$

$$R^2 = 1 - \frac{\sum_{i=1}^{n}(y_i - \hat{y}_i)^2}{\sum_{i=1}^{n}(y_i - \bar{y})^2} \tag{4}$$

where y_i, $\hat{y}_i$ and $\bar{y}$ are the measured, predicted, and averaged (over the actual values of considered data) values of elastic modulus, respectively and n represents the number of test data (between 3 and 5) in the training step and is 16 in the validation step. The flow diagram for the ANN program is shown in Fig. 2. To validate the quality of the trained model all 16 data obtained experimentally were used to confirm the predictive ability of the model.

The final predictive ANN model was used to investigate the influence of a wide range of compositions, fiber diameters and fiber orientations, presented in Table 2, on the elastic modulus of the electrospun PCL/gelatin membranes. The AI was determined based on the circumferential direction of the mandrel collector.

2.7. Sensitivity analysis

Determination of the relative importance of input variables is a technique for systematically changing the input variables in a model to determine the effects of such changes on the output of the model and to show how the input variables can be quantitatively apportioned [32]. The relative importance of various input factors on ANN simulations can be assessed by partitioning the hidden output connection weights into components connected with each input neuron [33,34]. The relative importance of input variables can be presented as [32]:

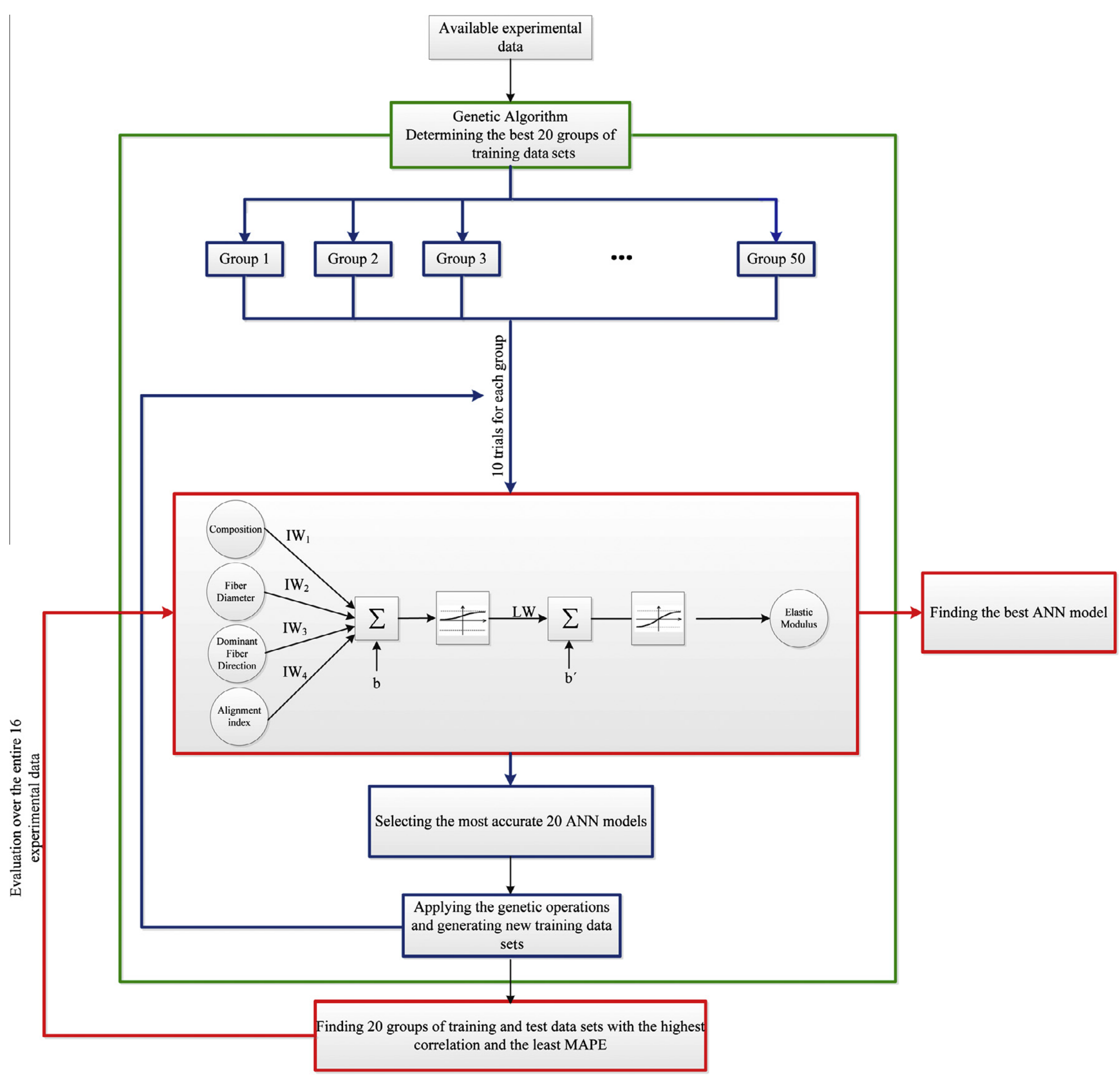

Fig. 2. Flow diagram for the developed ANN program.

Table 2
Range of applied input variables for prediction.

Composition (% PCL)	Fiber diameter (nm)	Alignment index	Alignment direction
30–90	270–1300	0.10–0.70	90

$$\text{Relative importance }(\%) = \frac{\sum_{j=1}^{n_H}\left[\left(i_{\upsilon j}/\sum_{k=1}^{n_\upsilon} i_{kj}\right)O_j\right]}{\sum_{i=1}^{n_\upsilon}\left[\sum_{j=1}^{n_H}\left(i_{\upsilon j}/\sum_{k=1}^{n_\upsilon} i_{kj}\right)O_j\right]} \times 100 \quad (5)$$

where n_υ and n_H are the number of neurons in the input and the hidden layers, respectively. i_j is the absolute value of connection weights between the input and the hidden layers, and O_j is the absolute value of connection weights between the hidden and the output layers. Altering parameters of greater calculated relative importance will have a bigger impact on the elastic modulus than altering parameters of smaller calculated relative importance [32].

3. Results

3.1. Morphological and mechanical assessment

The electrospun nanofibers were observed by SEM and the experimental results are summarized in Table 1. The AI for each sample is also included in Table 1. The results show that the fiber diameter increased with increasing solution concentration. Fig. 3 shows the distribution of fiber orientations for all 16 samples. It is suggested that changing the speed of the rotating mandrel from 50 to 1200 r.p.m. changes the fiber orientation to a nearly circumferential direction.

The elastic moduli of the fibers in both the longitudinal and circumferential directions were obtained under ambient and simulated physiological conditions. Table 3 shows that the mechanical properties of the scaffolds decreased upon exposure to simulated physiological conditions. The results indicate that the elastic modulus is sensitive to fiber orientation and fiber diameter, and at the same time these parameters are dependent on the conditions of electrospinning, including the concentration, weight ratio of the polymeric components and mandrel speed (Tables 1 and 3). The polymer composition has a direct impact on the mechanical properties, while the weight ratio of the polymeric components has an indirect effect on scaffold elasticity by influencing the fiber diameter and orientation.

3.2. Modeling topology and evaluation of the ANN prediction

The results of distinct models for each case are explained in this section. From among the different MAPE values that we obtained by our trial and error method (Table 4) the models with the lowest MAPE values (13.3–16.8%) signify the best topology and the best training method for each case, and also confirm the high accuracy of these models in predicting the elastic modulus. Table 5 shows the final samples that were selected by the GA as the test data set over the 16 experimental samples, with the aim of attaining a high accuracy prediction. Fig. 4 illustrates the network response versus the corresponding experimental results for the four presented models. Correlation coefficient values close to 1 (0.92–0.97) indicate a linear relationship between the experimentally determined and predicted elastic modulus in all cases, and yet again this confirms the predictive capability of our developed ANN models.

The experimental and predicted elastic modulus data are also shown in Fig. 5, where we observe reasonable agreement between the real and predicted data.

3.3. Sensitivity analysis

Fig. 6 shows the results of the sensitivity analysis, in which it was observed that "polymeric composition" remained the most sensitive parameter affecting the elastic modulus of the scaffold. This effect was greater for scaffolds tested under simulated physiological conditions. It can be also seen from Fig 6B that along the circumferential direction the effect of fiber orientation (44.5%) was almost as important as the effect of composition (42.0%). In addition, the relative importance of fiber diameter increased while that of fiber orientation decreased under simulated physiological conditions compared with its importance under ambient conditions.

3.4. Effect of input variables on the elastic modulus

Three-dimensional plots of the predicted values of elastic modulus corresponding to different input variables (Table 2) are displayed in Fig. 7. It not only shows the relation of elastic modulus to the structural properties of the scaffold, such as composition, fiber diameter and fiber orientation, but also illustrates a wide range of elastic modulus values that can be obtained from the same material by altering the composition and morphological features of the electrospun scaffold. According to our models electrospun PCL/gelatin scaffolds can have elastic modulus values in the range 1.0–140.0 MPa under ambient conditions, depending on the composition, diameter and orientation of the fibers, which are consistent with the values of elastic modulus reported in the literature. Various values of elastic modulus for different compositions and structures of electrospun PCL/gelatin scaffolds have been presented by other researchers (e.g. 10.3 MPa by Kai et al. [11], 28.7 MPa by Venugopal et al. [8], and 138.3 MPa by Heydarkhan-Hagvall et al. [10]). However, the results from the ANN models showed that the elastic modulus of the same scaffolds hydrated under simulated physiological conditions decreased to 0.5–15.0 MPa.

Fig. 8 summarizes the elastic moduli of various tissues, and suggests that electrospun PCL/gelatin scaffolds can be produced with varying elastic properties suitable for multiple TE applications [35–37].

4. Discussion

The mechanical properties of electrospun scaffolds on both micro and macro scales are crucial factors when designing scaffolds for tissue regeneration. On the micro scale the mechanical properties, especially scaffold stiffness, can influence cell migration, growth and differentiation [14,38–40]. The effect of the stiffness of an electrospun PCL scaffold on embryonic mesenchymal pluripotent cells was studied by Nam et al., who showed that the stiffness of the scaffolds significantly altered the gene expression of mesenchymal pluripotent cells during the early phase of chondrogenic and osteogenic differentiation [41]. Furthermore, the similarity of the scaffold elastic modulus to that of the target tissue is a key factor that determines the efficacy of the scaffold, ultimately influencing tissue regeneration.

The major challenge faced by bioengineers is to identify the process parameters that control the macro-mechanical properties of the scaffolds in order to closely match those of the tissue of concern. For electrospun scaffolds it is possible to achieve varying mechanical properties from a composite scaffold containing two polymers, by merely changing the polymer ratio, fiber diameter and fiber orientation. Plenty of research has been carried out into cellular responses to the polymer composition, diameter [42–44] and alignment [44–47] of electrospun fibers. However, it has rarely

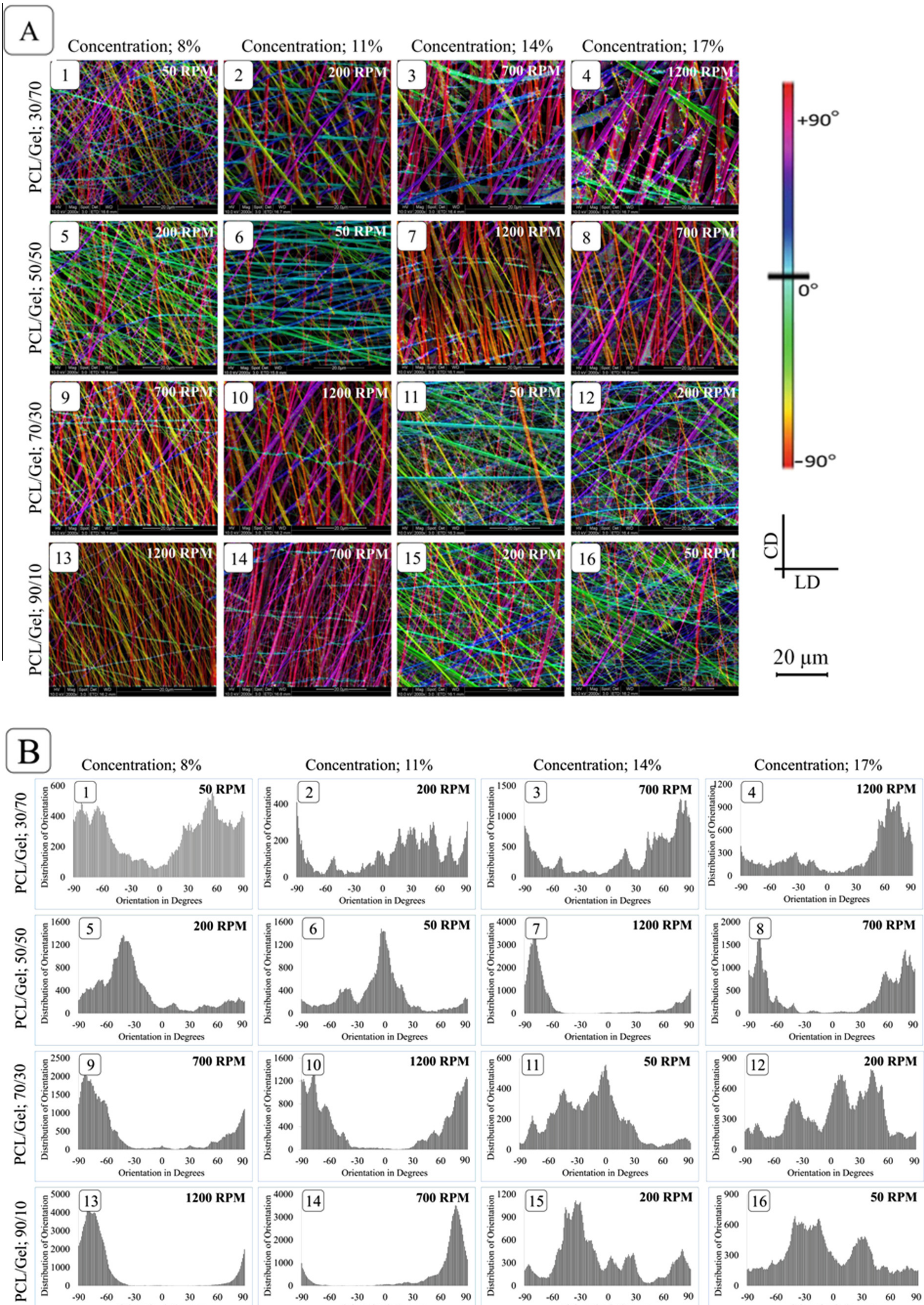

Fig. 3. Fiber orientation distribution as (A) a color coded map and (B) histograms. LD and CD refer to the longitudinal and circumferential directions, respectively.

Table 3
Measured elastic modulus of PCL/gelatin nanofibers under ambient and physiological conditions.

Sample	Elastic modulus (MPa)			
	Ambient conditions		Simulated physiological conditions	
	Longitudinal	Circumferential	Longitudinal	Circumferential
1	60.5 ± 4.8	44.9 ± 3.4	0.6 ± 0.4	0.7 ± 0.2
2	80.9 ± 3.9	55.6 ± 5.5	1.2 ± 0.3	1.0 ± 0.1
3	85.9 ± 7.8	102.8 ± 16.5	0.8 ± 0.3	1.2 ± 0.2
4	91.7 ± 15.6	122.3 ± 21.3	1.9 ± 0.7	2.6 ± 1.1
5	67.0 ± 11.8	42.5 ± 5.7	1.2 ± 0.4	1.7 ± 1.5
6	87.4 ± 15.5	49.4 ± 5.7	4.3 ± 1.4	1.4 ± 0.2
7	60.1 ± 6.7	134.6 ± 14.5	3.1 ± 0.6	5.4 ± 1.2
8	66.3 ± 10.2	58.8 ± 7.5	9.1 ± 1.2	5.5 ± 1.0
9	18.1 ± 3.1	52.6 ± 7.9	1.9 ± 0.6	5.1 ± 1.3
10	17.6 ± 3.0	77.1 ± 3.1	1.5 ± 0.3	8.2 ± 1.8
11	68.5 ± 9.7	30.7 ± 4.7	6.9 ± 1.5	3.3 ± 0.5
12	41.8 ± 14.6	46.5 ± 7.0	6.2 ± 0.8	6.8 ± 1.0
13	4.8 ± 0.8	28.7 ± 1.7	1.9 ± 0.1	15.6 ± 3.6
14	12.3 ± 1.9	52.9 ± 4.5	2.8 ± 1.3	12.5 ± 1.7
15	25.6 ± 1.4	20.8 ± 5.3	12.7 ± 1.4	8.7 ± 2.1
16	29.0 ± 4.1	21.5 ± 3.7	11.8 ± 1.7	7.3 ± 1.5

Table 4
Evaluation of ANN models with different architectures.

Mode	No. of hidden layers	No. of neurons in each layer	Transfer functions		Training method	MAPE (%)
			Hidden layers	Output layers		
Am-L	1	3	Logsig	Tansig	RP	30.4
Am-L	1	10	Logsig	Purelin	LM	69.7
Am-L	1	10	Tansig	Logsig	LM	47.6
Am-L	2	3–5	Tansig-purelin	Logsig	RP	58.5
Am-L[a]	1	1	Logsig	Tansig	LM	13.3
Am-C	1	3	Logsig	Tansig	LM	34.0
Am-C	1	3	Logsig	Tansig	SCG	45.7
Am-C	1	1	Purelin	Tansig	SCG	25.7
Am-C[a]	1	1	Logsig	Tansig	LM	14.3
SP-L	1	1	Purelin	Logsig	LM	27.9
SP-L	2	1–1	Tansig-tansig	Tansig	LM	22.1
SP-L	2	2–3	Purelin-tansig	Purelin	LM	77.2
SP-L[a]	1	1	Logsig	Tansig	LM	16.8
SP-C	1	3	Logsig	Tansig	RP	60.2
SP-C	2	2–3	Purelin-tansig	Tansig	SCG	36.7
SP-C[a]	1	1	Logsig	Tansig	LM	14.5

L, longitudinal direction; C, circumferential directions; Am, ambient conditions; SP, simulated physiological conditions; Purelin, linear; Tansig, hyperbolic tangent sigmoid; Logsig, log-sigmoid.
[a] Optimum ANN model.

Table 5
Final training and test data sets obtained using the developed genetic algorithm.

Case	Final samples used as the test data set
Ambient longitudinal	6, 7, 12, 14
Ambient circumferential	3, 7, 12, 14
Simulated physiological longitudinal	2, 8, 9, 16
Simulated physiological circumferential	8, 11, 13, 14

been stated that such effects might be due to the specific mechanical properties of the scaffolds with which the cells closely interacted. Therefore, in this study we focused on investigating the effect of compositional polymeric ratios and the morphology of electrospun PCL/gelatin scaffolds on their mechanical properties, especially their elasticity. In the present study we fabricated electrospun scaffolds of varying fiber diameter and fiber orientation by altering the electrospinning parameters.

Tong and Wang applied a factorial design approach to determine the most critical parameters of electrospinning that influence the fiber diameter and alignment [48]. Following a similar perspective we changed the polymeric concentration and the rotation speed of the collector (mandrel) to obtain fibers with varying diameters and orientations, respectively. A Taguchi L'16 orthogonal array was applied during this study, and the membranes were electrospun under 16 different conditions. The weight ratio of the polymers (PCL:gel), total concentration and mandrel rotation speed at four levels were the parameters chosen to prepare 16 samples differing in composition, fiber diameter and fiber orientation. The Taguchi method was used to reduce the number of experiments by testing pairs of combinations instead of having to test all possible combinations of variables. As shown in Table 1, for each composition used in this study the fiber diameter increased as the total concentration of the polymer increased, which can be attributed to the increased viscosity of the polymeric solution. We gradually increased the polymer concentration from 8% to 17% and mandrel rotation speed from 50 to 1200 r.p.m. to investigate the effect of fiber diameter and fiber orientation on the elastic modulus of the electrospun scaffolds. It is known that solutions with a lower polymer concentration produce fibers of smaller diameter, while an increased collector rotation speed gives more

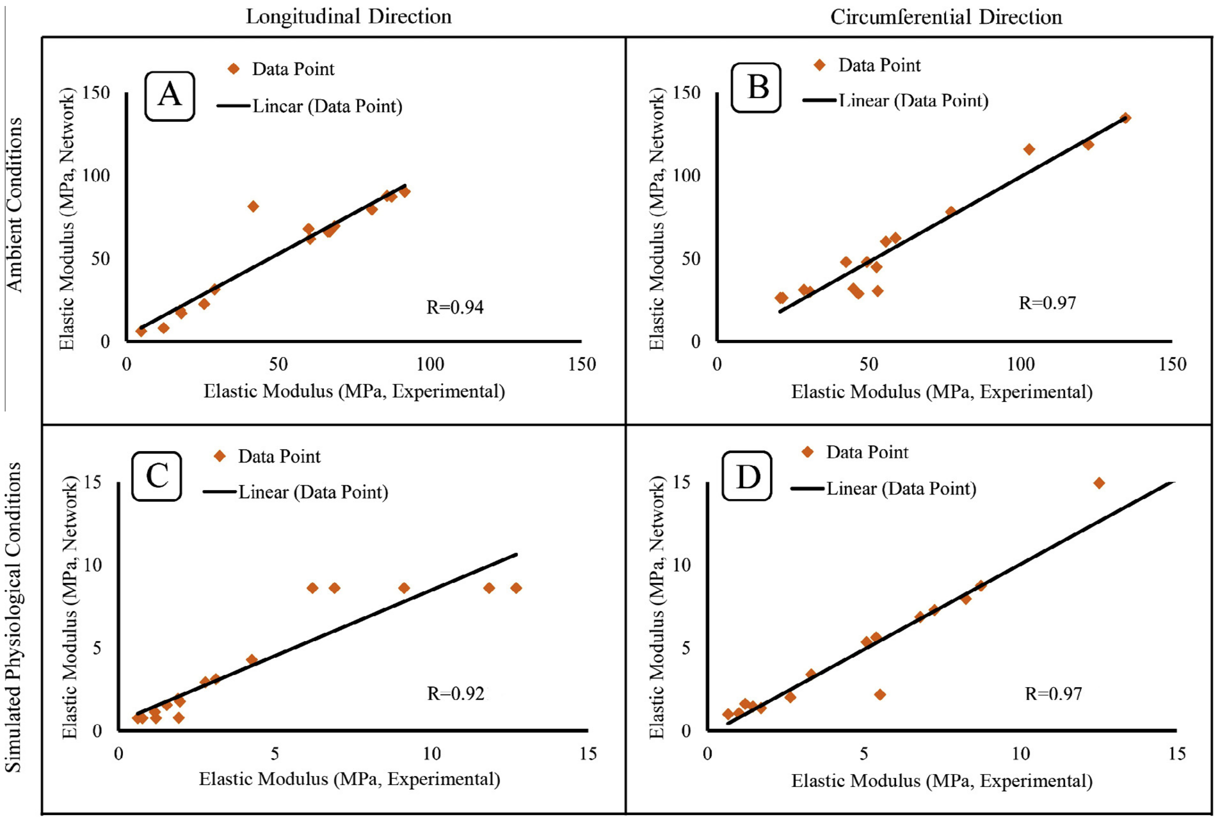

Fig. 4. Regression analysis between ANN responses and the experimental results for (A) the longitudinal and (B) the circumferential elastic moduli under ambient conditions and for (C) the longitudinal and (D) the circumferential elastic moduli under simulated physiological conditions.

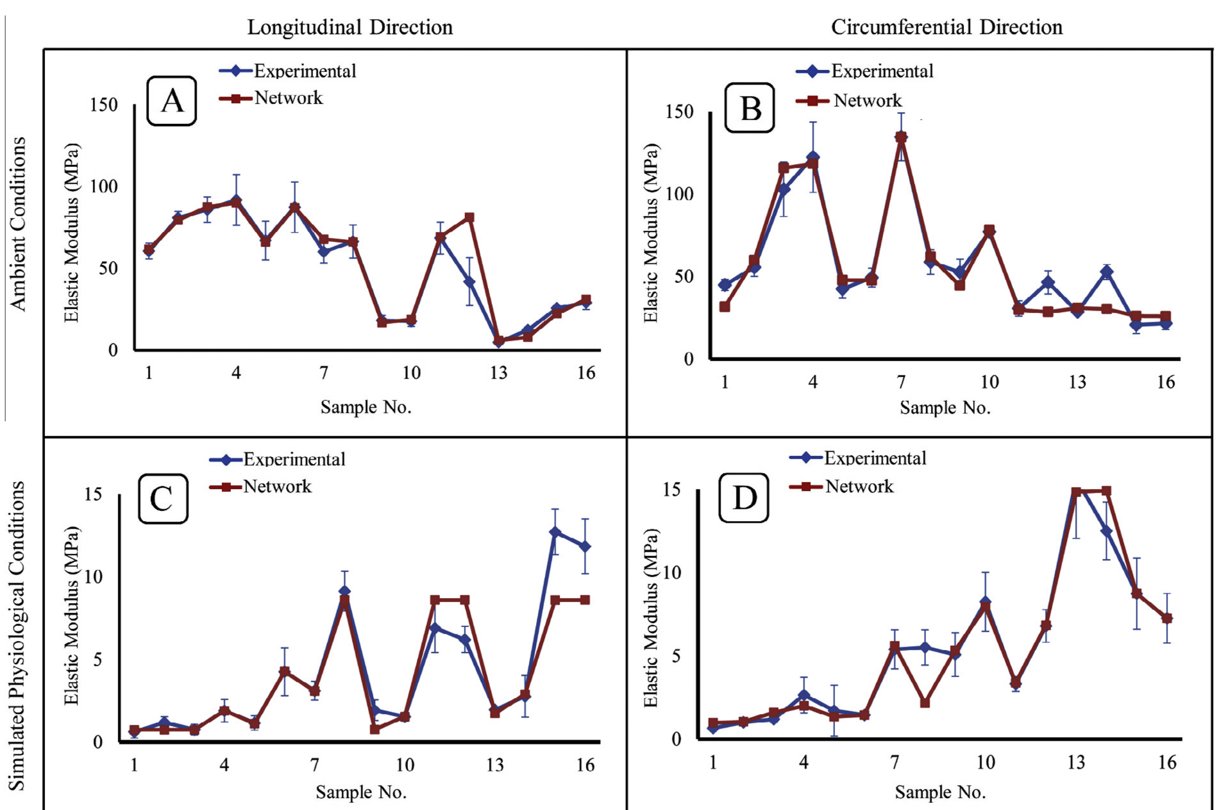

Fig. 5. Experimentally measured and predicted values of the elastic modulus under ambient conditions in (A) the longitudinal and (B) the circumferential directions and under simulated physiological conditions in (C) the longitudinal and (D) the circumferential directions.

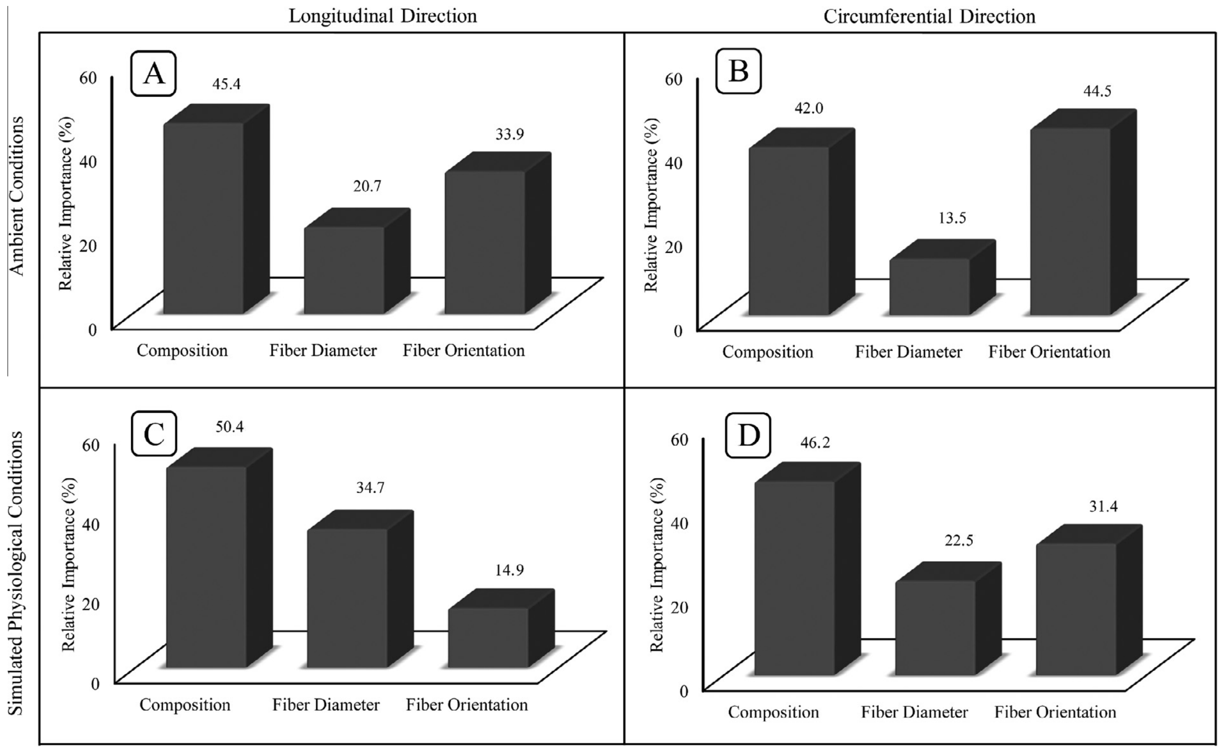

Fig. 6. Relative effects of the parameters on the elastic modulus under ambient conditions in (A) the longitudinal and (B) the circumferential directions and under simulated physiological conditions in (C) the longitudinal and (D) the circumferential directions.

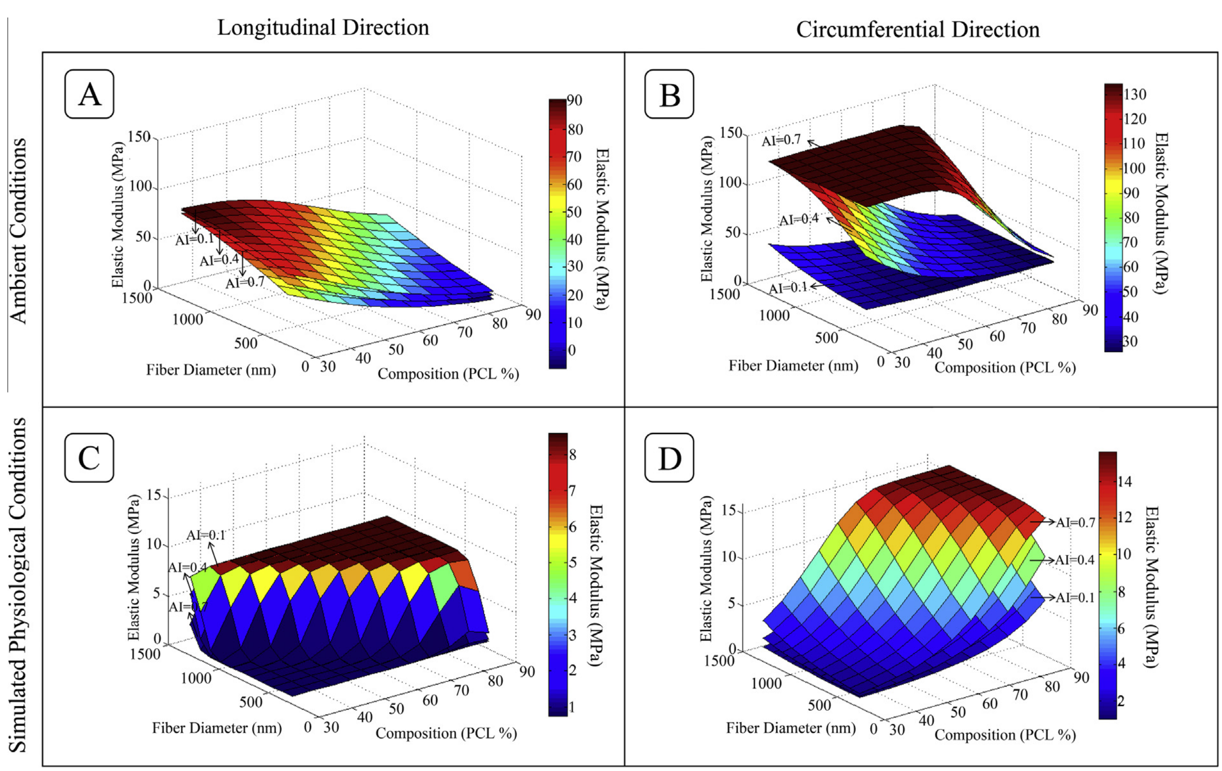

Fig. 7. Three-dimensional plots of elastic moduli predicted by the ANN models for AI = 0.1, 0.4, and 0.7 in (A) the longitudinal and (B) the circumferential directions under ambient conditions and in (C) the longitudinal and (D) the circumferential directions under simulated physiological conditions.

circumferentially aligned fibers. We observed that the degree of alignment of fibers collected at the same rotation speed depends on the solution parameters (Fig. 3). The ratio of the two polymers might also influence the degree of fiber alignment. Ghasemi-Mobarakeh et al. reported that with increasing gelatin content in electrospun PCL/gelatin scaffolds the probability of fiber breakage

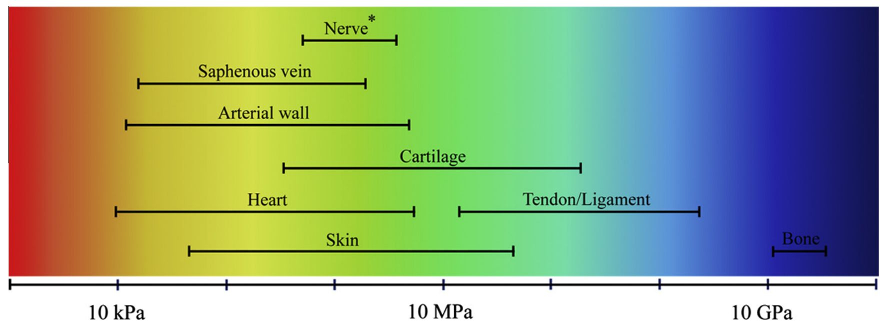

Fig. 8. Ranges of elastic moduli of various natural tissues [35,36]*[37].

increased due to a decrease in solution viscosity and, therefore, the fiber alignment also decreased [5]. Similar observations were also made by Schnell et al. using a blend of PCL and collagen [49]. Increasing the gelatin content in a solution of PCL/gelatin reduced the fiber diameter upon electrospinning under the same conditions. This phenomenon was also observed for electrospun poly (L-lactide-co-ε-caprolactone) (PLCL)/gel, poly(lactic-co-glycolic acid) (PLGA)/gelatin and polyglycolic acid (PGA)/gelatin scaffolds [5,50–52]. This is mainly because of the increased amino acid content in the solution upon increasing the concentration of gelatin, which resulted in a higher charge density, greater self-repulsion and improved stretching of the jet during the electrospinning process [51]. These results indicate that although the fiber diameter and orientation are mainly influenced by the polymer solution concentration and the rotation speed of the mandrel, respectively, they are also affected by the amount of gelatin within the polymeric composition. Such interactions between the parameters introduce complexity, especially in determining the conditions required to produce the best structure with an appropriate elastic modulus. It was therefore difficult or impractical to accurately reach general conclusions using limited experimental results and, hence, developing a modeling strategy can simplify the general prediction of macro-mechanical properties in terms of the compositional and structural features of electrospun membranes.

The ANN is a valuable tool for modeling linear and nonlinear phenomena. The principle behind this approach is to replicate the biological structures and functions of the brain. ANN learning is based on examples and generalizing the acquired knowledge [53]. The multilayer feed forward neural network, also known as a multilayer perceptron (MLP), is the most common neural network architecture used to solve nonlinear regression problems. One of the popular training algorithms for feed forward neural networks is BP, which is an iterative optimization process where the performance function is minimized by adjusting the weights appropriately. The weights and biases are iteratively updated in the direction in which the performance function decreases most rapidly [16]. The Levenberg–Marquardt method used in this study is often the fastest BP algorithm and is highly recommended as a first choice supervised algorithm, although it requires more memory than other algorithms [54]. The optimal architecture of the ANN model, including the number of hidden layers and neurons and the transfer functions in each layer, along with the training method, was determined based on the minimum MAPE values for the training and test data sets by trial and error. In this work an ANN model consisting of one hidden layer with one neuron and log-sigmoid and hyperbolic tangent sigmoid transfer functions in the hidden and output layers, respectively, was the optimal network structure for all cases. Because the efficiency of ANN models is based on the accuracy of prediction, we used the MAPE values and linear correlation coefficients to evaluate the predictive power of the developed models. From the graphs of actual vs. predicted values of elastic modulus shown in Figs. 4 and 5 along with the MAPE values reported in Table 4 it can be seen that the ANN models developed in the present study had a linear correlation coefficient of 0.92–0.97 and MAPE values of 13.3–16.8%, with fairly good levels of prediction accuracy, which verified proper design of the models developed to successfully forecast the elasticity of electrospun scaffolds with respect to their composition, fiber diameter and fiber orientation in both the longitudinal and circumferential directions under either ambient or simulated physiological conditions. To the best of our knowledge there is very limited information available in the literature regarding this effect and this is the first study of its kind that clearly identifies the simultaneous impact of structural characteristics of the electrospun scaffolds and compares the relative importance of composition, fiber diameter and fiber orientation for the elasticity characteristics of electrospun scaffolds under both ambient and simulated physiological conditions.

Figs. 6 and 7 demonstrate that the compositional ratio of the polymers constituting the fibers is the most effective parameter affecting the elastic modulus of the scaffolds under both ambient and simulated physiological conditions. PCL is an elastic polymer [55], while gelatin is a stiff and brittle biopolymer [50], and their blending ratios can affect the elastic modulus of the final constructs. The amount of gelatin within the fibers affects the fiber diameter and its alignment, eventually influencing the elastic modulus of the resultant scaffold. As shown in Fig. 6, the importance of polymer composition was greater under the simulated physiological conditions than under ambient conditions and reached 50.4% and 46.2% for the longitudinal and circumferential directions, respectively. Thus the elastic modulus under simulated physiological conditions is more sensitive to the compositional ratio of polymers. This confirms the need for attention in choosing appropriate compositions of the polymers in order to obtain scaffolds with the desired mechanical properties under physiological conditions. The increased effect of polymeric composition on the elastic modulus observed under simulated physiological conditions can be assigned to the behavior of "gelatin" under hydrating conditions. Under hydrating cindirions gelatin contributes significantly to water adsorption as well as mass loss by scaffolds in comparison with its behavior under dry conditions. Along the circumferential direction, in addition to polymeric composition, fiber orientation was found to have a remarkable effect on the elastic modulus under ambient conditions. The relative importance of fiber orientation to the elasticity of the scaffolds under ambient conditions was 33.9% and 44.5% along the longitudinal and circumferential directions, respectively, and dropped to 14.9% and 31.4% after hydration. This decreased effect might be due to swelling of the fibers under simulated physiological conditions owing to water adsorption by gelatin, which might also influence the fiber orientation.

Moreover, the fiber diameter of a scaffold affects the pore size and the effect is more significant under hydrated conditions due to the varying water absorption capabilities of fibers with different pore sizes. For to these reasons the importance of fiber diameter under simulated physiological conditions increased from 20.7% to 34.7% and from 13.5% to 22.5%, along the longitudinal and circumferential directions, respectively.

Fig. 6A and B illustrates the greater importance of fiber orientation along the circumferential direction compared with its effect along the longitudinal direction, which means a defined change in fiber orientation caused a larger change in circumferential elastic modulus than longitudinal elastic modulus. The relative importance of fiber orientation and fiber diameter is dependent on two mechanisms: (i) the angle between the fibers and the loading direction dictated by fiber orientation, determines the contribution of each individual fiber to the overall elastic modulus of the electrospun scaffold; (ii) junctions and entanglements between the fibers [13,56]. The strength and number of fiber junctions are dependent on the fiber diameter and orientation, with the intensity of fiber junctions decreasing with increasing fiber alignment (i.e. AI) [57]. Therefore fiber orientation can affect the elastic modulus through both mechanisms, which also indicates the greater importance of this parameter than fiber diameter under ambient conditions.

Fibers oriented parallel to the direction of loading were tensile loaded at the same time and made the greatest contribution to load bearing, leading to a higher elastic modulus along the circumferential direction [58]. The lowest contribution of fibers was observed when the stress was applied perpendicular to the aligned fibers, which results in a decreased elastic modulus of the electrospun scaffold along the longitudinal direction. The results of our modeling studies show that the effect of fiber diameter on the elastic modulus along the longitudinal direction is greater than its effect along the circumferential direction. From among the scaffolds with nearly aligned fibers, highly compact scaffolds will have a higher elastic modulus. At the same time, relating the compactness of scaffolds to their diameter, the porosity of the electrospun mats increased with decreasing fiber diameter, which means that scaffolds with finer fibers have a more porous structure with a lower packing density [59]. This phenomenon might be more persistent when stress is applied along the longitudinal direction (perpendicular to the aligned fibers), thus resulting in greater importance of fiber diameter along the longitudinal direction than along the circumferential direction. We set a maximum rotation speed of 1200 r.p.m. for the collector to achieve stable electrospinning, and obtained a highest AI of 0.7, indicating the co-existence of random fibers along with aligned fibers. The fiber angle with respect to load bearing and fiber junctions also dominate in influencing the elastic modulus of random fibers. Thus it is clear that the elastic modulus of electrospun random and aligned PCL/gelatin scaffolds depends on both the above described mechanisms.

Fiber diameter was the more effective factor with a greater effect under simulated physiological conditions while the effect of fiber diameter under ambient conditions was not pronounced compared with the effect of composition and fiber orientation. Although fiber diameter was the least important parameter influencing scaffold elasticity, it had a greater impact on the longitudinal elastic modulus of hydrated scaffolds than fiber orientation, because of the combined roles of loading direction and hydration conditions. The results of our models (Fig. 7) also revealed that aligned nanofibrous scaffolds showed anisotropic mechanical behavior consistent with their architectural anisotropy, similar to other studies [14,60]. The longitudinal and circumferential elastic moduli of the aligned fibers (AI = 0.7) lie in the range 1.0–90.0 MPa and 30.0–135.0 MPa, respectively (Fig. 7A and B), which confirms the anisotropic behavior of the aligned fibers. On the other hand, no significant differences in the elastic moduli of random fibers (AI = 0.1) were observed along the longitudinal direction compared with the circumferential direction, which confirms the isotropic behavior of the random fibers.

Random fibers had a lower elastic modulus than aligned fibers measured along the circumferential direction. This can be attributed to the angle between the random fibers and the applied force, which caused the fibers to experience rotation upon loading, while the aligned fibers stretched uniaxially with less fiber rotation [61]. It has been demonstrated that the elastic modulus is proportional to the diameter of the fibers, which is attributed to the higher packing density of nanofibers with increasing fiber diameter. Since increased diameters correspond to an increase in fiber packing density (or in other words fiber volume fraction), more fibrous elements are available for mechanical loading, which results in a greater elastic modulus [60]. In addition, scaffolds with larger fiber diameters have stronger junctions, which results in increased elastic moduli [15].

Electrospun scaffolds were exposed to simulated physiological conditions for 24 h because supposedly, cells seeded on scaffolds attach within 24 h and start to secrete ECM components, providing additional mechanical support to the regenerating tissue. Thus the importance of scaffold mechanical properties during the early stage of cell seeding was prioritized in this study. Based on our findings the elastic modulus of the electrospun scaffolds dropped markedly under simulated physiological conditions, by an average of 80%. Our results highlight the importance of paying more attention to the mechanical properties of the scaffolds under simulated physiological conditions when considering them for TE applications, rather than under ambient conditions. A huge decrease (80%) in the elastic modulus of scaffolds under simulated physiological conditions was also demonstrated by Kai et al. for electrospun PCL/gelatin (50:50) scaffolds [11]. Despite a knowledge of the detrimental effects of hydrating conditions on the scaffold elastic modulus, electrospun PCL/gelatin scaffolds, especially with a 50:50 compositional ratio, have been widely applied in TE to provide structural integrity and mechanical properties to injured tissues. Gelatin, being a natural polymer, might weaken the scaffolds upon hydration, leading to a significant decrease in elastic modulus. Similar results have been reported for electrospun PLGA/gelatin and cellulose acetate/gelatin scaffolds used for cardiac and skin TE, respectively [62,63].

Beyond the effect of structural parameters on the elastic modulus, the most important application of the proposed model is its ability to be combined with other optimization methods for reverse engineering of scaffolds to determine the required structural properties and to fabricate scaffolds with mechanical properties comparable with the target regenerating tissue. It is worth mentioning that under in vivo conditions tissues are subjected to multiaxial stresses, however, uniaxial tensile testing is usually used to evaluate the mechanical properties of bioengineered scaffolds, due to its simplicity. The ANN approach is also capable of modeling the multi-axial mechanical properties of structures, which has not been explored in this study. The quantitative predictions of the proposed models are only applicable to electrospun PCL/gelatin scaffolds, however, the qualitative results are general and extendable to other compositions.

5. Conclusion

The relationship between the compositional ratio, fiber diameter and fiber orientation of electrospun PCL/gelatin membranes and their elasticity as an index of mechanical performance under ambient and simulated physiological conditions are discussed. The ANN-based model is a powerful tool to predict the elastic modulus of electrospun scaffolds over a wide range of fiber diameters and fiber orientations in addition to different compositions, using a limited set of experiments which were designed using a robust method, the Taguchi method. The results suggest that electrospun PCL/gelatin can be successfully engineered for regeneration of various soft tissues that require different mechanical properties.

Acknowledgements

This research was supported by a NRF-Technion grant (R-398-001-065-592) and the Nanoscience and Nanotechnology Initiative, Faculty of Engineering, National University of Singapore, Singapore.

Appendix Figures. with essential colour discrimination

Certain figures in this article, particularly Figures 1–5, 7 and 8, are difficult to interpret in black and white. The full colour images can be found in the on-line version, at http://dx.doi.org/10.1016/j.actbio.2013.09.015.

References

[1] Andrady AL. Science and technology of polymer nanofibers. New York: John Wiley & Sons; 2008.

[2] Chen ZG, Wang PW, Wei B, Mo XM, Cui FZ. Electrospun collagen–chitosan nanofiber: a biomimetic extracellular matrix for endothelial cell and smooth muscle cell. Acta Biomater 2010;6:372–82.

[3] Subia B, Kundu J, Kundu SC. Biomaterial scaffold fabrication techniques for potential TE applications. In: Eberli D, editor. Tissue engineering. Vienna: In-Tech; 2010. p. 141–57.

[4] Reneker DH, Hou H. Electrospinning. In: Wnek GE, Bowlin GL, editors. Encyclopedia of biomaterials and biomedical engineering. Zug: Informa Healthcare; 2008. p. 978–85.

[5] Ghasemi-Mobarakeh L, Prabhakaran MP, Morshed M, Nasr-Esfahani M-H, Ramakrishna S. Electrospun poly(epsilon-caprolactone)/gel nanofibrous scaffolds for nerve TE. Biomaterials 2008;29:4532–9.

[6] Zeugolis DI, Khew ST, Yew ESY, Ekaputra AK, Tong YW, Yung L-YL, et al. Electro-spinning of pure collagen nano-fibres – just an expensive way to make gelatin? Biomaterials 2008;29:2293–305.

[7] Chong EJ, Phan TT, Lim IJ, Zhang YZ, Bay BH, Ramakrishna S, et al. Evaluation of electrospun PCL/gel nanofibrous scaffold for wound healing and layered dermal reconstitution. Acta Biomater 2007;3:321–30.

[8] Venugopal JR, Low S, Choon AT, Kumar AB, Ramakrishna S. Nanobioengineered electrospun composite nanofibers and osteoblasts for bone regeneration. Artif Organs 2008;32:388–97.

[9] Alvarez-Perez MA, Guarino V, Cirillo V, Ambrosio L. Influence of gelatin cues in PCL electrospun membranes on nerve outgrowth. Biomacromolecules 2010;11:2238–46.

[10] Heydarkhan-Hagvall S, Schenke-Layland K, Dhanasopon AP, Rofail F, Smith H, Wu BM, et al. Three-dimensional electrospun ECM-based hybrid scaffolds for cardiovascular TE. Biomaterials 2008;29:2907–14.

[11] Kai D, Prabhakaran MP, Jin G, Ramakrishna S. Guided orientation of cardiomyocytes on electrospun aligned nanofibers for cardiac TE. J Biomed Mater Res B 2011;98B:379–86.

[12] Xiang P, Li M, Zhang C-Y, Chen D-L, Zhou Z-H. Cytocompatibility of electrospun nanofiber tubular scaffolds for small diameter TE blood vessels. Int J Biol Macromol 2011;49:281–8.

[13] Li W-J, Mauck RL, Cooper JA, Yuan X, Tuan RS. Engineering controllable anisotropy in electrospun biodegradable nanofibrous scaffolds for musculoskeletal TE. J Biomech 2007;40:1686–93.

[14] Stylianopoulos T, Bashur CA, Goldstein AS, Guelcher SA, Barocas VH. Computational predictions of the tensile properties of electrospun fibre meshes: effect of fibre diameter and fibre orientation. J Mech Behav Biomed Mater 2008;1:326–35.

[15] Milleret V, Simona B, Neuenschwander P, Hall H. Tuning electrospinning parameters for production of 3D-fiber-fleeces with increased porosity for soft TE. Eur Cells Mater 2011;21:286–303.

[16] Khayet M, Cojocaru C, Essalhi M. Artificial neural network modeling and response surface methodology of desalination by reverse osmosis. J Membrane Sci 2011;368:202–14.

[17] Faridi-Majidi R, Ziyadi H, Naderi N, Amani A. Use of artificial neural networks to determine parameters controlling the nanofibers diameter in electrospinning of nylon-6,6. J Appl Polym Sci 2012;124:1589–97.

[18] Lou WG, Nakai S. Application of artificial neural networks for predicting the thermal inactivation of bacteria: a combined effect of temperature, pH and water activity. Food Res Int 2001;34:573–9.

[19] Costolo MA, Lennhoff JD, Pawle R, Rietman EA, Stevens AE. A nonlinear system model for electrospinning sub-100 nm polyacrylonitrile fibres. Nanotechnology 2008:19.

[20] Nateri AS, Hasanzadeh M. Using fuzzy-logic and neural network techniques to evaluate polyacrylonitrile nanofiber diameter. J Comput Theor Nanos 2009;6:1542–5.

[21] Nasouri K, Bahrambeygi H, Rabbi A, Shoushtari AM, Kaflou A. Modeling and optimization of electrospun PAN nanofiber diameter using response surface methodology and artificial neural networks. J Appl Polym Sci 2012;126:127–35.

[22] Sarkar K, Ben Ghalia M, Wu Z, Bose SC. A neural network model for the numerical prediction of the diameter of electro-spun polyethylene oxide nanofibers. J Mater Process Tech 2009;209:3156–65.

[23] Rabbi A, Nasouri K, Bahrambeygi H, Shoushtari AM, Babaei MR. RSM and ANN approaches for modeling and optimizing of electrospun polyurethane nanofibers morphology. Fiber Polym 2012;13:1007–14.

[24] Dev VRG, Venugopal JR, Senthilkumar M, Gupta D, Ramakrishna S. Prediction of water retention capacity of hydrolysed electrospun polyacrylonitrile fibers using statistical model and artificial neural network. J Appl Polym Sci 2009;113:3397–404.

[25] Majumdar PK, Majumdar A. Predicting the breaking elongation of ring spun cotton yarns using mathematical, statistical, and artificial neural network models. Text Res J 2004;74:652–5.

[26] Behera BK, Muttagi B. Comparative analysis of modeling methods for predicting woven fabric properties. J Text Eng 2005;51:1–9.

[27] Hadizadeh M, Jeddi AAA, Tehran MA. The prediction of initial load-extension behavior of woven fabrics using artificial neural network. Text Res J 2009;79:1599–609.

[28] Hedayat AS, Sloane NJA, Stufken J. Orthogonal arrays: theory and applications. New York: Springer Verlag; 1999.

[29] Roy RK. Design of experiments using the taguchi approach: 16 steps to product and process improvement. New York: John Wiley & Sons; 2001.

[30] Fonck E, Feigl GG, Fasel J, Sage D, Unser M, Rufenacht DA, et al. Effect of aging on elastin functionality in human cerebral arteries. Stroke 2009;40:2552–6.

[31] Rezakhaniha R, Agianniotis A, Schrauwen JTC, Griffa A, Sage D, Bouten CVC, et al. Experimental investigation of collagen waviness and orientation in the arterial adventitia using confocal laser scanning microscopy. Biomech Model Mech 2012;11:461–73.

[32] Rezakazemi M, Razavi S, Mohammadi T, Nazari AG. Simulation and determination of optimum conditions of pervaporative dehydration of isopropanol process using synthesized PVA-APTEOS/TEOS nanocomposite membranes by means of expert systems. J Membrane Sci 2011;379:224–32.

[33] Garson DG. Interpreting neural-network connection weights. AI Expert 1991;6:46–51.

[34] Goh ATC. Seismic liquefaction potential assessed by neural networks. J Geotech Eng 1994;120:1467–80.

[35] Nemir S, West JL. Synthetic materials in the study of cell response to substrate rigidity. Ann Biomed Eng 2010;38:2–20.

[36] Kim H, Kang D-H, Kim M, Jiao A, Kim D-H, Suh K-Y. Patterning methods for polymers in cell and TE. Ann Biomed Eng 2012;40:1339–55.

[37] Masaeli E, Morshed M, Nasr-Esfahani MH, Sadri S, Hilderink J, van Apeldoorn A, et al. Fabrication, characterization and cellular compatibility of poly(hydroxy alkanoate) composite nanofibrous scaffolds for nerve TE. Plos One 2013;8:e57157.

[38] Engler AJ, Sen S, Sweeney HL, Discher DE. Matrix elasticity directs stem cell lineage specification. Cell 2006;126:677–89.

[39] Levy-Mishali M, Zoldan J, Levenberg S. Effect of scaffold stiffness on myoblast differentiation. Tissue Eng Part A 2009;15:935–44.

[40] Discher DE, Ivanovska I, Buxboim A. Matrix elasticity directs stem cell fates – how deeply can cells feel? In: ElHaj A, Bader D, editors. 8th International conference on cell & stem cell engineering (ICCE, Ireland): Springer Berlin Heidelberg; 2011. p. 21–22.

[41] Nam J, Johnson J, Lannutti JJ, Agarwal S. Modulation of embryonic mesenchymal progenitor cell differentiation via control over pure mechanical modulus in electrospun nanofibers. Acta Biomater 2011;7:1516–24.

[42] Moroni L, Licht R, de Boer J, de Wijn JR, van Blitterswijk CA. Fiber diameter and texture of electrospun PEOT/PBT scaffolds influence human mesenchymal stem cell proliferation and morphology, and the release of incorporated compounds. Biomaterials 2006;27:4911–22.

[43] Chen M, Patra PK, Warner SB, Bhowmick S. Role of fiber diameter in adhesion and proliferation of NIH 3T3 fibroblast on electrospun polycaprolactone scaffolds. Tissue Eng 2007;13:579–87.

[44] Bashur CA, Shaffer RD, Dahlgren LA, Guelcher SA, Goldstein AS. Effect of fiber diameter and alignment of electrospun polyurethane meshes on mesenchymal progenitor cells. Tissue Eng Part A 2009;15:2435–45.

[45] Xu CY, Inai R, Kotaki M, Ramakrishna S. Aligned biodegradable nanotibrous structure: a potential scaffold for blood vessel engineering. Biomaterials 2004;25:877–86.

[46] Yang F, Murugan R, Wang S, Ramakrishna S. Electrospinning of nano/micro scale poly(L-lactic acid) aligned fibers and their potential in neural TE. Biomaterials 2005;26:2603–10.

[47] Chew SY, Mi R, Hoke A, Leong KW. The effect of the alignment of electrospun fibrous scaffolds on Schwann cell maturation. Biomaterials 2008;29:653–61.

[48] Tong H-W, Wang M. An investigation into the influence of electrospinning parameters on the diameter and alignment of poly(hydroxybutyrate-co-hydroxyvalerate) fibers. J Appl Polym Sci 2011;120:1694–706.

[49] Schnell E, Klinkhammer K, Balzer S, Brook G, Klee D, Dalton P, et al. Guidance of glial cell migration and axonal growth on electrospun nanofibers of poly-

epsilon-caprolactone and a collagen/poly-epsilon-caprolactone blend. Biomaterials 2007;28:3012–25.
[50] Lee J, Tae G, Kim YH, Park IS, Kim S-H, Kim SH. The effect of gelatin incorporation into electrospun poly(l-lactide-co-ε-caprolactone) fibers on mechanical properties and cytocompatibility. Biomaterials 2008;29:1872–9.
[51] Meng ZX, Wang YS, Ma C, Zheng W, Li L, Zheng YF. Electrospinning of PLGA/gel randomly-oriented and aligned nanofibers as potential scaffold in TE. Mater Sci Eng C 2010;30:1204–10.
[52] Hajiali H, Shahgasempour S, Naimi-Jamal MR, Peirovi H. Electrospun PGA/gel nanofibrous scaffolds and their potential application in vascular TE. Int J Nanomed 2011;6:2133–41.
[53] Trebar M, Susteric Z, Lotric U. Predicting mechanical properties of elastomers with neural networks. Polymer 2007;48:5340–7.
[54] Rostamizadeh M, Rizi SMH. Predicting gas flux in silicalite-1 zeolite membrane using artificial neural networks. J Membrane Sci 2012;403:146–51.
[55] McClure MJ, Sell SA, Simpson DG, Walpoth BH, Bowlin GL. A three-layered electrospun matrix to mimic native arterial architecture using polycaprolactone, elastin, and collagen: a preliminary study. Acta Biomater 2010;6:2422–33.
[56] Prabhakaran MP, Vatankhah E, Ramakrishna S. Electrospun aligned PHBV/collagen nanofibers as substrates for nerve TE. Biotechnol Bioeng 2013;97:529–38.
[57] D'Amore A, Stella JA, Wagner WR, Sacks MS. Characterization of the complete fiber network topology of planar fibrous tissues and scaffolds. Biomaterials 2010;31:5345–54.
[58] Hong SG, Kim GH. Mechanically improved electrospun PCL biocomposites reinforced with a collagen coating process: preparation, physical properties, and cellular activity. Bioprocess Biosyst Eng 2013;36:205–14.
[59] Soliman S, Sant S, Nichol JW, Khabity M, Traversa E, Khademhosseini A. Controlling the porosity of fibrous scaffolds by modulating the fiber diameter and packing density. J Biomed Mater Res A 2011;96:566–574.
[60] Thomas V, Jose MV, Chowdhury S, Sullivan JF, Dean DR, Vohra YK. Mechano-morphological studies of aligned nanofibrous scaffolds of polycaprolactone fabricated by electrospinning. J Biomater Sci Polym Ed 2006;17:969–84.
[61] Zhang S. Mechanical and physical properties of electrospun nanofibers. Raleigh, NC: North Carolina State University; 2009.
[62] Prabhakaran MP, Kai D, Ghasemi-Mobarakeh L, Ramakrishna S. Electrospun biocomposite nanofibrous patch for cardiac TE. Biomed Mater 2011;6:055001.
[63] Vatankhah E, Prabhakaran MP, Jin G, Ghasemi Mobarakeh L, Ramakrishna S. Development of nanofibrous cellulose acetate/gel skin substitutes for variety wound treatment applications. J Biomater Appl 2013.